



Ultralow-temperature superplasticity and its novel mechanism in ultrafine-grained Al alloys

Nguyen Q. Chinh, Maxim Yu Murashkin, Elena V. Bobruk, János L. Lábár, Jenő Gubicza, Zsolt Kovács, Anwar Q. Ahmed, Verena Maier-Kiener & Ruslan Z. Valiev

To cite this article: Nguyen Q. Chinh, Maxim Yu Murashkin, Elena V. Bobruk, János L. Lábár, Jenő Gubicza, Zsolt Kovács, Anwar Q. Ahmed, Verena Maier-Kiener & Ruslan Z. Valiev (2021) Ultralow-temperature superplasticity and its novel mechanism in ultrafine-grained Al alloys, *Materials Research Letters*, 9:11, 475-482, DOI: [10.1080/21663831.2021.1976293](https://doi.org/10.1080/21663831.2021.1976293)

To link to this article: <https://doi.org/10.1080/21663831.2021.1976293>



© 2021 The Author(s). Published by Informa UK Limited, trading as Taylor & Francis Group



[View supplementary material](#)



Published online: 15 Sep 2021.



[Submit your article to this journal](#)



[View related articles](#)



[View Crossmark data](#)

Ultralow-temperature superplasticity and its novel mechanism in ultrafine-grained Al alloys

Nguyen Q. Chinh ^a, Maxim Yu Murashkin ^{b,c}, Elena V. Bobruk ^{b,c}, János L. Lábár ^a, Jenő Gubicza ^a, Zsolt Kovács ^a, Anwar Q. Ahmed ^a, Verena Maier-Kiener ^d and Ruslan Z. Valiev ^{b,c}

^aDepartment of Materials Physics, Eötvös Loránd University, Budapest, Hungary; ^bInstitute of Physics of Advanced Materials, Ufa State Aviation Technical University, Ufa, Russia; ^cLaboratory for Mechanics of Bulk Nanomaterials, Saint Petersburg State University, St. Petersburg, Russia;

^dDepartment of Physical Metallurgy and Materials Testing, Leoben University, Leoben, Austria

ABSTRACT

The important benefits of ultrafine-grained (UFG) alloys for various applications stem from their enhanced superplastic properties. However, decreasing the temperature of superplasticity and providing superplastic forming at lower temperatures and higher strain rates is still a priority. Here, we disclose, for the first time, the mechanism by which grain boundary sliding and rotation are enhanced, when UFG materials have grain boundary segregation of specific alloying elements. Such an approach enables achieving superplasticity in commercial Al alloys at ultralow homologous temperatures below 0.5 (i.e. below 200°C), which is important for developing new efficient technologies for manufacturing complex-shaped metallic parts with enhanced service properties.

IMPACT STATEMENT

For the first time, ultralow-temperature superplasticity is found in commercial 7xxx Al alloy. This discovery enables the development of new technologies for the superplastic forming of complex-shaped products with enhanced service properties.

ARTICLE HISTORY

Received 10 June 2021

KEYWORDS

Ultralow-temperature superplasticity; aluminum alloys; ultrafine-grained materials; severe plastic deformation; high-pressure torsion

1. Introduction

Superplasticity of materials is an important field of scientific research both because it presents significant challenges in the areas of flow mechanisms and because it forms the underlying basis for the commercial superplastic forming industry in which complex shapes and curved parts are formed from superplastic metals [1,2].

It is well established that two basic requirements must be fulfilled in order to achieve superplastic flow. First, superplasticity requires a very small grain size, typically smaller than $\sim 10 \mu\text{m}$. Second, superplasticity is a diffusion-controlled process operating with grain boundary (GB) sliding – as the main flow mechanisms – and therefore, it requires a relatively high testing temperature typically at or above $\sim 0.7\text{--}0.8 \times T_m$, where T_m is the absolute melting temperature of the material. At the same time, the developments of metallic materials during the last two decades with ultrafine grains of nanosized range by means of severe plastic deformation (SPD) processing paved the way towards new discoveries in the field of superplasticity [3,4]. Actually, the basic relationship for

superplasticity has the form:

$$\dot{\varepsilon} = \frac{ADGb}{kT} \left(\frac{b}{d}\right)^q \left(\frac{\sigma}{G}\right)^{1/m} \quad (1)$$

where $\dot{\varepsilon}$ is the strain rate of the deformation process, D is the appropriate diffusion coefficient, G is the shear modulus, b is the magnitude of the Burgers vector, k is Boltzmann's constant, T is the absolute temperature, d is the grain size, σ is the applied stress, q is the exponent of the inverse grain size, m is the strain rate sensitivity, and A is a dimensionless constant [1,2,5]. The temperature dependence of the superplastic deformation is mainly determined by the diffusion coefficient, based on the formula

$$D = D_0 \exp\left(\frac{-Q}{RT}\right) \quad (2)$$

where D_0 is a frequency factor, Q is the activation energy, and R is the universal gas constant.

Based on Equation (1), the formation of ultrafine grains in the nanosized range provides an opportunity

CONTACT Nguyen Q. Chinh chinh@metal.elte.hu; Ruslan Z. Valiev ruslan.valiev@ugatu.su

Supplemental data for this article can be accessed here. <https://doi.org/10.1080/21663831.2021.1976293>

to control the temperature and the rate of superplastic flow in materials, which are quite attractive for the practical application of their superplastic forming. In recent years, this problem has been actively discussed in the literatures [6–11].

In the present paper, the new GB approach is for the first time investigated and demonstrated for an Al–Zn–Mg–Zr aluminum alloy. This widely used age-hardenable alloy of the Al–Zn–Mg (7xxx) series with multi-alloying elements was chosen due to fact that, it is the one of the basic materials in the aluminum industry. These alloys are generally used after conventional treatments and, as having an average grain size of 5–10 μm , they can be deformed superplastically for a total elongation of 300–500%, but only at a high temperature of about 500°C ($\sim 0.8 \times T_m$) [1,5]. The work presented here reports a unique grain boundary behavior controlled by GB segregations in an ultrafine-grained Al–Zn–Mg–Zr alloy, which can be deformed superplastically with a record total elongation of 500% in a temperature region lower than 170°C ($0.47 \times T_m$).

2. Materials and methods

Briefly, the alloy with a composition of Al–2.04at%Zn–1.37at%Mg–0.04at%Zr (or well-known as Al–4.8wt%Zn–1.2wt%Mg–0.14wt%Zr) was processed high-pressure torsion (HPT). The HPT process is described in detail elsewhere [12]. The microstructure of the HPT-processed sample was investigated using transmission electron microscope (TEM), energy-disperse X-ray spectroscopy (EDS) and scanning transmission electron microscope (STEM) with high-angle annular dark-field (HAADF) detector.

Strain rate sensitivity of the investigated samples were determined by indentation creep [13]. Mechanical properties of the samples were followed by microhardness and tensile tests.

More information on both materials and methods can be found in the supplemental material.

3. Results and discussion

As a result of HPT, a saturated UFG microstructure having an average grain size of 200 nm was produced, as shown in Figure 1(a).

Before performing tensile tests, the thermal stability and the strain rate sensitivity of the HPT-processed sample were studied in order to predict its ductility in the low-temperature region between 120°C and 170°C. After

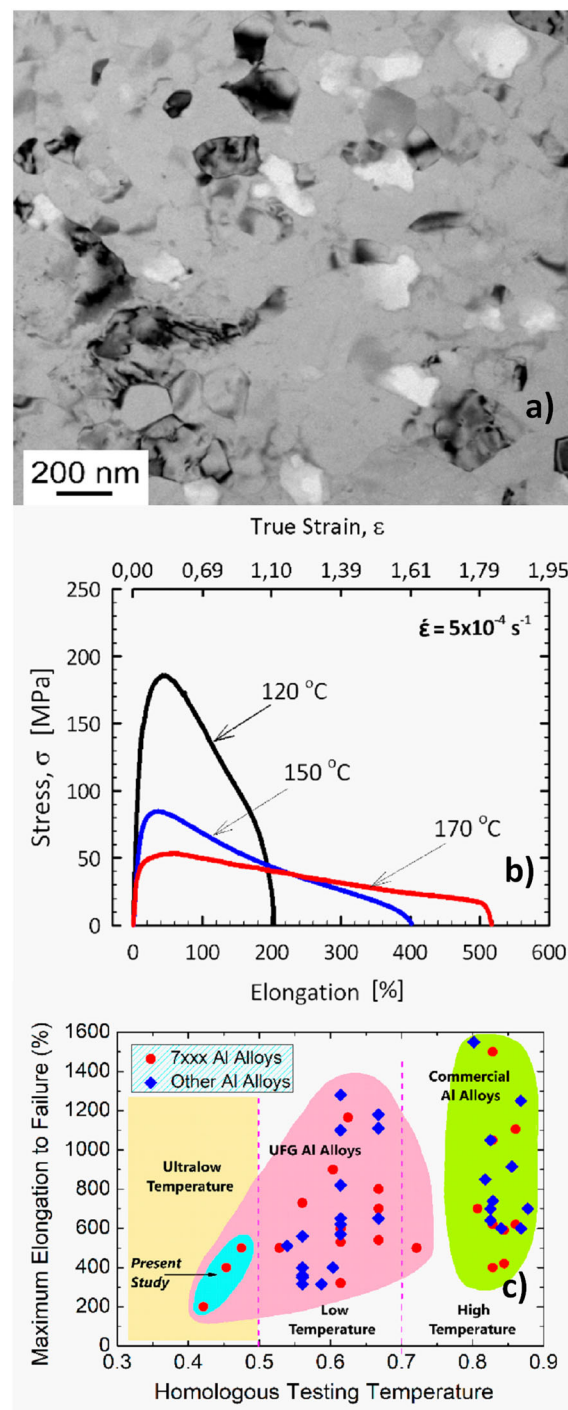


Figure 1. Characteristics of ultralow-temperature superplasticity in the UFG Al–Zn–Mg–Zr alloy: (a) UFG structure having an average grain size of ~ 200 nm, (b) Stress–strain (σ – ϵ) curves, showing a total elongation higher than 500% at 170°C (0.47 homologous temperature) and (c) Significance of the present study indicated by reviewing the temperature dependence of superplasticity of commercial Al alloys of 7000 (AlZnMg-based) system [5,15–24] and other (AlMg-, AlLi-based) systems [1,7,15,25–30].

annealing the HPT-processed sample for 2 h at 120°C, the average grain size was practically unchanged, and it increased only to about 300 nm at 170°C, showing a stable UFG structure in this sample [14]. An unusually high strain rate sensitivity, m , of 0.43 ± 0.02 was obtained by using nanoindentation creep test in the same temperature region, indicating that superplasticity can be expected at low temperatures.

Samples were deformed by tension at different strain rates and different temperatures lower than $0.5 \times T_m$. Figure 1(b) shows the typical stress–strain curves of superplastic deformation taken at a strain rate of $\dot{\epsilon} = 5 \times 10^{-4} \text{ s}^{-1}$ at 120°C, 150°C and 170°C. It can be seen that a total elongation of almost 200% is obtained at a very low temperature of 120°C ($\sim 0.42 \times T_m$), and a record deformation higher than 500% was observed at 170°C ($\sim 0.47 \times T_m$).

The significance of the new experimental results is illustrated in the summary graph shown in Figure 1(c), where the maximum elongation of about 400% and higher for several commercial Al alloys can be seen as a function of the homologous testing temperature. The literature data on previous 7xxx (Al–Zn–Mg-based) and other (mainly Al–Mg- and Al–Li-based) Al alloys can be found in only two temperature ranges. Conventional commercial Al alloys, which usually contain Zr and/or Sc as the grain-refining elements, having average grain size of $1 - 10 \mu\text{m}$, can typically be superplastically deformed in the high (> 0.7) temperature range. Ultrafine-grained (UFG) Al alloys with lower average grain size of $100 - 700 \text{ nm}$ show superplastic behavior mainly in the low homologous temperature between 0.5 and 0.7. For lower homologous temperature, in the ultralow region, there are only data from the present research. It is obvious that our new results (see in Figure 1(c)) present a record total elongation of 500% in the ultralow-temperature region, at a homologous temperature of 0.47 and total elongation of 400% at $0.45 T_m$.

In order to explain the new, unique experimental results, the characteristics of the deformation process were studied. The activation energy, Q , of the deformation process, characterizing the superplastic flow, is determined by using Equations (1 and 2) in another form:

$$\dot{\epsilon} = B \cdot \sigma^{1/m} \cdot \exp\left(\frac{-Q}{RT}\right) \quad (3)$$

which describes the stress- and temperature dependence of the strain rate. In Equation (3), B is a constant depending on the properties of material. Taking the stress values at the same elongation of 100% ($\epsilon = 0.69$) for different testing temperatures, using the value of 0.43 for m obtained by indentation creep, from the slope of the

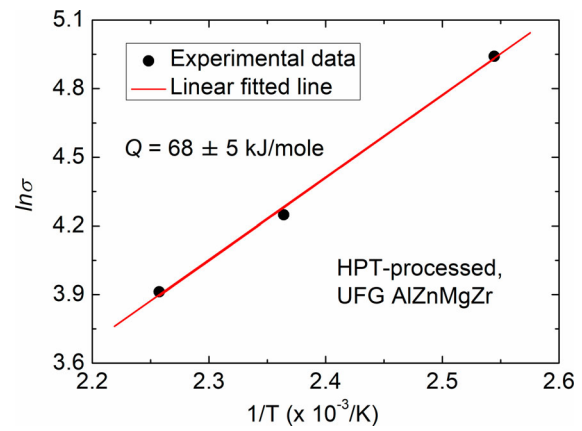


Figure 2. Determination of the activation energy (Q) of ultralow-temperature superplasticity in the UFG Al–Zn–Mg–Zr alloy.

$\ln \sigma - 1/T$ line, a value of 68 kJ/mole can be estimated for the activation energy, Q , as demonstrated in Figure 2.

Considering both the high strain rate sensitivity and the relative stability of the microstructure of the sample during deformation, the basic mechanism of the superplastic deformation of the investigated UFG alloy should certainly be grain boundary sliding. The experimentally determined activation energy of 68 kJ/mole is lower than the values for self-diffusion in Al (142 kJ/mole) [31] or grain boundary diffusion in Al (84 kJ/mole) [31]. In order to explain the occurrence and significance of the experimentally obtained activation energy, let us examine the microstructure of the superplastically deformed samples.

Figure 3(a) shows a HAADF image obtained by STEM on the sample deformed superplastically for a total elongation higher than 500% at 170°C. Besides the MgZn_2 phase particles, which appear as bright areas on the image since the atomic number of Zn is much higher than that of Al, Zn-rich Al/Al grain boundaries indicated by small green arrows can also be observed. A small area of the image marked with a white dashed square is shown with a higher magnification in Figure 3(b) and analyzed by using energy-dispersive X-ray spectroscopy (EDS) mapping in Figure 3(c–f).

The EDS results reveal clearly the depletion of Al (see Figure 3(c)), and the excess of Mg and Zn atoms (shown in Figure 3(d,e), respectively) in the Al/Al grain boundaries of this HPT-processed UFG sample. EDS measurements at different locations also show that the fractions of Zn and Mg change along the grain boundaries, and there are places where Zn atoms are the main contributors to the excess solute atoms in the Al/Al grain boundaries, while in other locations the concentration of Mg is higher than that of Zn. In every case, the matrix grain boundaries of this UFG sample can be regarded as Zn/Mg-rich boundaries. For instance, Figure 3(f) reveals that the sum

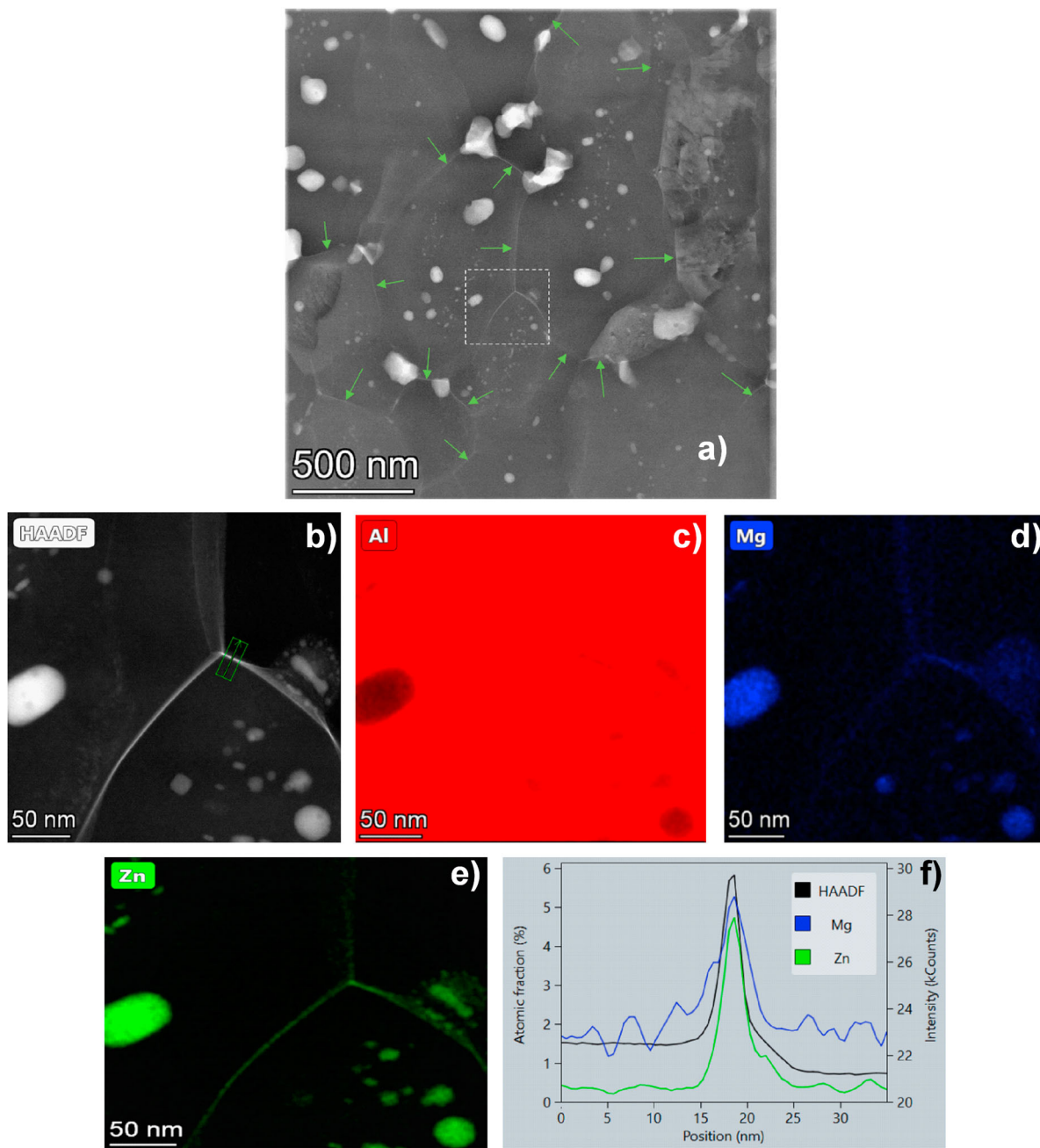


Figure 3. Microstructure of the sample superplastically deformed at 170°C and a strain rate of $5 \times 10^{-4} \text{ s}^{-1}$ (a) Low magnification STEM-HAADF image showing the existence of Zn-containing particles (bright ones) and Zn-rich Al/Al grain boundaries (indicated by the green arrows), (b) High magnification HAADF image showing Zn-rich grain boundaries (forming a brightly imaged triple junction). (c–e) corresponding EDS maps for Al, Mg and Zn, respectively. (f) EDS line profile analysis along a boundary, marked by arrows in the HAADF image, showing the segregation of Zn and Mg atoms into Al/Al grain boundaries in the HPT-processed UFG sample.

of Zn and Mg concentrations in the boundary reached about 10 at.%.

The segregation of solute atoms to the grain boundaries in an HPT-processed supersaturated solid solution was recently interpreted by numerical and analytical calculations [32]. During the SPD process, after reaching a saturated UFG microstructure, the role of the grain boundaries is enhanced in subsequent deformation

processes due to the significance of grain boundary sliding [3,9,33]. It was shown in the mentioned numerical calculations that GBS can relax the external shear stress during SPD, forming an inhomogeneous stress field around the sliding grain boundaries [32]. The hydrostatic component (p) of this stress field may induce up-hill diffusion currents, leading to accumulation sites for both vacancies and solute atoms at the grain boundaries. It

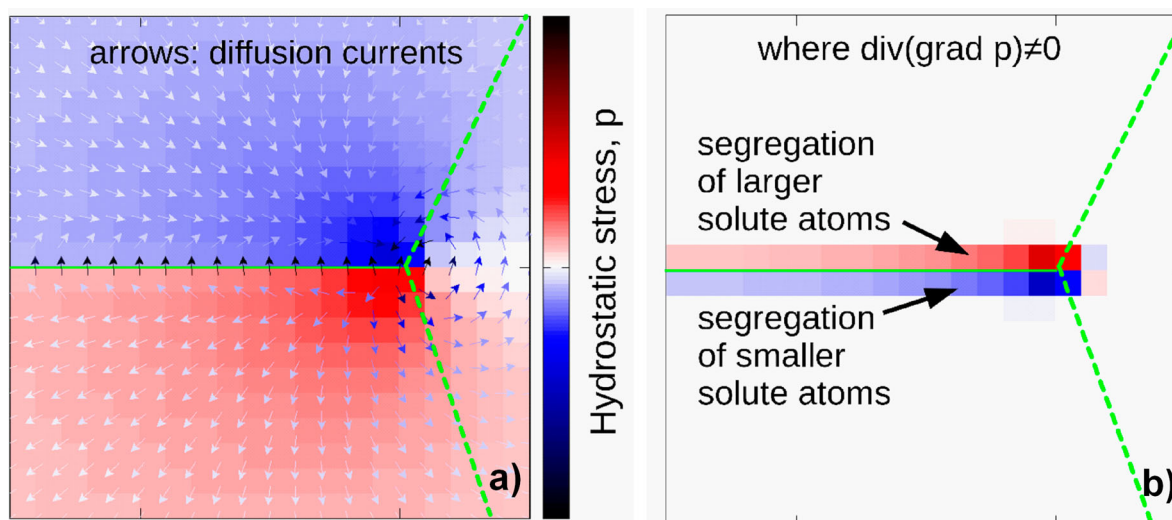


Figure 4. Trapping effect of sliding grain boundary. (a) Calculated hydrostatic stress component (p) around a slipped grain boundary (the arrows show the direction of the diffusion currents). (b) Accumulation points for solute atoms smaller (red) and larger (blue) than the matrix atoms (Al). The green dashed lines represent the grain boundaries.

should be noted that the mentioned hydrostatic component causes different currents for different volume-size solute atoms. According to the theoretical calculation, Figure 4 shows an example demonstrating the trapping effect of a sliding boundary for larger (e.g. Mg) and smaller (e.g. Zn) solute atoms (compared to the Al matrix) at the opposite sides of the sliding grain boundary. Considering the EDS line profiles for Zn and Mg shown in Figure 3(f), the segregation of the solute atoms with different sizes along the grain boundary seems to be experimentally confirmed.

The strong segregation of Zn to the matrix grain boundaries is already a known phenomenon in high-Zn concentrated model binary Al–Zn alloys with a UFG structure [34–38], but it has not been reported yet for the 7xxx series Al alloys. This is a key point in the observed ultralow-temperature superplasticity for the present UFG Al–Zn–Mg–Zr alloy. Since superplasticity is based on grain boundary diffusion, it is worth to calculate the diffusion coefficient, D , using the formula (2). For grain boundary diffusion in both pure Al and Zn, the values of D_0 are similar and lie between $\sim 1.3 \times 10^{-14}$ and $\sim 5 \times 10^{-14} \text{ m}^2 \text{ s}^{-1}$, as shown in a previous study [31]. Using the activation energy of $Q = 84 \text{ kJ/mole}$ for grain boundary diffusion of Al at $T = 443 \text{ K}$ (corresponding to 170°C) [31], it follows that the diffusion coefficient, D , may be estimated to be between 1.60×10^{-24} and $6.16 \times 10^{-24} \text{ m}^2 \text{ s}^{-1}$. Applying the experimentally determined activation energy of 68 kJ/mole , the value of D can be found between 1.23×10^{-22} and $4.74 \times 10^{-22} \text{ m}^2 \text{ s}^{-1}$ at 170°C , which is almost two orders of magnitude

higher than the aforementioned values calculated for grain boundary diffusion in Al.

According to both experimental and simulation results shown in Figures 3 and 4, respectively, the HPT-processed Al–Zn–Mg–Zr sample can be regarded as a two-phase system comprising a grain interior phase and a thin layer grain boundary phase enriched in Zn and Mg. Considering the Al–Zn binary phase diagram, the addition of Zn to Al yields a lower temperature of melting. Similar effect can be observed when Mg is added to Al. For relatively low Zn and Mg concentrations, 1 at.% solute addition results in a reduction of the solidus temperature with 8.3 and 13 K, respectively. The solidus temperature can be considered as a quasi-melting point of the grain boundary phase. Thus, for the grain boundary composition shown in Figure 3(f), the concentrations of Zn and Mg (4 and 6 at.%, respectively) can cause more than 100 K reduction of the melting point. Due to the lower melting point, the testing temperatures between 120°C and 170°C corresponded to an elevated homologous temperature higher than 0.5 during deformation with GBS. Indeed, for fcc crystals, the activation energy of grain boundary diffusion is proportional with the melting point and the proportionality constant is $0.078 \text{ kJ}/(\text{mole}\cdot\text{K})$ [39]. Using the estimated melting point of the grain boundary phase (about 830 K), 65 kJ/mole is calculated for the activation energy of grain boundary diffusion, which agrees with the measured value within the experimental error ($68 \pm 5 \text{ kJ/mole}$). The higher quasi-homologous temperature is certainly an important factor that resulted in higher activation of

grain boundary sliding and thereby contributed highly to the excellent superplasticity. As noted above, in the model UFG Al–Zn alloy an enhanced GBS and a high ductility are observed even during deformation at RT.

Considering separately the segregation of Zn and Mg solutes to grain boundaries, it should be noted that both the experimental results (see Figure 3(f)) and recent theoretical calculations [40] reveal a significant difference between the profiles of these atoms across the grain boundary. While a relatively broad segregation having 5–6 nm half-width can be observed for Mg, a much thinner Zn layer with 2–3 nm half-width formed at the boundary shown in Figure 3. This is due to the extra effect of the electronic structure in the case of Zn, as *3d* element [40]. Because of the broad segregation, the promoting effect of Mg addition on the deformation in the grain boundaries due to the reduction of the quasi-melting point can be lowered or even suppressed by the hindering effect of the large Mg atoms on the dislocation motion. Dislocation glide acts as a complementary mechanism beside grain boundary diffusion during superplastic deformation since the change of the grain shape can occur with the help of dislocation slip. Therefore, the broadly distributed Mg atoms with large size hinder the dislocation motion effectively in the vicinity of grain boundaries, thereby hindering the occurrence of superplastic deformation. Recent atomic simulations of Koju and Mishin [41] also have shown that Mg segregation at grain boundaries may hinder GBS. Indeed, superplasticity has not been observed in ultrafine-grained Al–Mg solid solutions without Zn addition. If the effect of Mg on the melting point depression in the grain boundaries is neglected, the Zn segregation alone yields a grain boundary activation energy of about 70 kJ/mole (see the previous paragraph for the fundamentals of this calculation) which is also close to the experimentally determined activation energy of the superplastic deformation for the present alloy (68 kJ/mole). Thus, it is the grain boundary segregation of Zn, rather than Mg, that is responsible for the accelerated diffusion and enhanced sliding, which are necessary conditions for the occurrence of superplasticity at lower temperatures.

The significant advantage of ultralow-temperature superplasticity is, on the one hand, the potential energy savings during low-temperature deformation, and on the other hand, the preservation of the fine-grained microstructure. Experimental results have shown that, as can be seen in Figure 3(a), the microstructure of the sample after superplastic deformation at 170°C remains equiaxial and ultrafine with an average grain size of about 400 nm. Similarly, to the effect of static annealing, MgZn₂ phase small precipitates with a size between 10 and 70 nm were formed inside the grains during

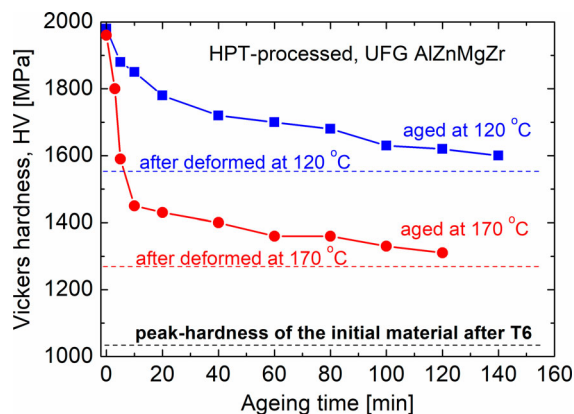


Figure 5. The room temperature Vickers hardness (HV) of the samples after superplastic deformation at 120°C (blue dashed line) and 170°C (red dashed line), as well as the peak hardness obtained for the initial coarse-grained sample after the conventional T6 treatment (black dashed line). The hardness values of the HPT-processed UFG samples statically annealed for different times at 120°C (blue solid square) and 170°C (red solid circle) are also plotted to show the thermal stability of this sample.

deformation at 170°C. Owing to both the ultrafine grain size and the strengthening particles, the material retains its high strength even after superplastic deformation, as shown in Figure 5, where the room temperature hardness of the HPT-processed and the superplastically deformed UFG samples can be seen and compared with the peak hardness of the initial coarse-grained sample.

It is well established that the so-called T6 conventional heat treatment must be applied to the 7xxx series alloys for producing the maximum strength [42,43]. This treatment conventionally includes the aging at 120°C for 24 h of quenched and supersaturated samples, resulting in the maximum strengthening effect of precipitates. In the present case, the peak hardness of the initial sample after the T6 treatment is ~1020 MPa. It can be seen that the hardness values of the samples after superplastic deformation (1280 and 1560 MPa at 170°C and 120°C, respectively) are still 20–50% higher than the mentioned peak hardness of the initial sample after the conventional T6 treatment.

Summarizing the above, the performed research demonstrates for the very first time the possibility of extremely low-temperature superplasticity in traditional Al alloys of the 7xxx series. The origin of this effect is related to the formation, through SPD processing, of an UFG structure where Zn segregations are present at grain boundaries, providing accelerated diffusion and enhanced sliding at lower temperatures. The discovery of the low-temperature superplasticity creates an opportunity for the development of new technologies

for the superplastic forming of complex-shaped products exhibiting a high structural strength in operating conditions at room temperature.

Data availability

The data that support the findings of this study are all own results of the authors, not available anywhere.

Disclosure statement

No potential conflict of interest was reported by the author(s).

Funding

This research was supported by the Hungarian-Russian bilateral Research program (TÉT) No. 2017-2.3.4-TÉT-RU-2017-00005. This work was completed in the ELTE Institutional Excellence Program (TKP2020-IKA-05) financed by the Hungarian Ministry of Human Capacities. R.Z.V. and M.Y.M. acknowledge the support in part from the Russian Foundation for Basic Research (RFBR) (project No. 20-03-00614) and in part from the Ministry of Science and Higher Education of the Russian Federation under grant agreement No. 0838-2020-0006.

ORCID

Nguyen Q. Chinh  <http://orcid.org/0000-0002-6610-7308>

Maxim Yu Murashkin  <http://orcid.org/0000-0001-9950-0336>

Elena V. Bobruk  <http://orcid.org/0000-0001-8226-9887>

János L. Lábár  <http://orcid.org/0000-0002-3944-8350>

JenJenő Gubicza  <http://orcid.org/0000-0002-8938-7293>

Zsolt Kovács  <http://orcid.org/0000-0001-6802-3311>

Anwar Q. Ahmed  <http://orcid.org/0000-0002-8112-5694>

Verena Maier-Kiener  <http://orcid.org/0000-0003-1232-6078>

Ruslan Z. Valiev  <http://orcid.org/0000-0003-4340-4067>

References

- Nich TG, Wadsworth J, Sherby OD. Superplasticity in metals and ceramics. Cambridge: Cambridge University Press; 1997.
- Langdon TG. Seventy-five years of superplasticity: historic developments and new opportunities. *J Mater Sci.* 2009;44:5998–6010.
- Valiev R. Nanostructuring of metals by severe plastic deformation for advanced properties. *Nature Mater.* 2004;3:511–516.
- Valiev RZ, Estrin Y, Horita Z, et al. Fundamentals of superior properties in bulk nanoSPD materials. *Mater Res Lett.* 2016;4:1–21.
- Kaibyshev OA. Superplasticity of alloys, intermetallics and ceramics. Berlin: Springer-Verlag; 1992.
- Kawasaki M, Langdon TG. Review: achieving superplastic properties in ultrafine-grained materials at high temperatures. *J Mater Sci.* 2016;51:19–32.
- McFadden SX, Mishra RS, Valiev RZ, et al. Low-temperature superplasticity in nanostructured nickel and metal alloys. *Nature.* 1999;398:684–686.
- Ovid'ko IA, Valiev RZ, Zhu YT. Review on superior strength and enhanced ductility of metallic nanomaterials. *Prog Mater Sci.* 2018;94:462–540.
- Demirtas M, Purcek G. Room temperature superplasticity in fine/ultrafine grained materials subjected to severe plastic deformation, overview. *Mater Trans.* 2019;60:1159–1167.
- Demirtasa M, Kawasaki M, Yanar H, et al. High temperature superplasticity and deformation behavior of naturally aged Zn-Al alloys with different phase compositions. *Mater Sci Eng A.* 2018;730:73–83.
- Zhang YD, Jin S, Trimby PW, et al. Dynamic precipitation, segregation and strengthening of an Al-Zn-Mg-Cu alloy (AA7075) processed by high-pressure torsion. *Acta Mater.* 2019;162:19–32.
- Valiev RZ, Zhilyaev AP, Langdon TG. Bulk nanostructured materials: fundamentals and applications. Hoboken (NJ): John Wiley & Sons, Inc.; 2013.
- Chinh NQ, Szommer P. Mathematical description of indentation creep and its application for the determination of strain rate sensitivity. *Mater Sci Eng A.* 2014;611:333–336.
- Gubicza J, El-Tahawy M, Lábár JL, et al. Evolution of microstructure and hardness during artificial aging of an ultrafine-grained Al-Zn-Mg-Zr alloy processed by high pressure torsion. *J Mater Sci.* 2020;55:16791–16805.
- Charit I, Mishra RS. Low temperature superplasticity in a friction-stir-processed ultrafine grained Al-Zn-Mg-Sc alloy. *Acta Mater.* 2005;53:4211–4223.
- Lee S, Watanabe K, Matsuda K, et al. Low-temperature and high-strain-rate superplasticity of ultrafine-grained A 7075 processed by high-pressure torsion. *Mater Trans.* 2018;59:1341–1347.
- Liu FC, Ma ZY. Low-temperature superplasticity of friction stir processed Al-Zn-Mg-Cu alloy. *Scripta Mater.* 2008;58:667–670.
- Juhász A, Chinh NQ, Tasnádi P, et al. Superplasticity of aluminium alloys grain-refined by zirconium. *J Mater Sci.* 1987;22:137–143.
- Chinh NQ, Illy J, Juhasz A, et al. Mechanical Properties and superplasticity of AlZnMg alloys with copper and zirconium additions. *Phys Stat Sol.* 1995;149:583–599.
- Kotov AD, Mikhaylovskaya AV, Portnoy VK. Effect of the solid-solution composition on the superplasticity characteristics of Al-Zn-Mg-Cu-Ni-Zr alloys. *Phys Metal Metallogr.* 2014;115:730–735.
- Duan YI, Xu GF, Peng XY, et al. Effect of Sc and Zr additions on grain stability and superplasticity of the simple thermal-mechanical processed AlZnMg alloy sheet. *Mater Sci Eng A.* 2015;648:80–91.
- Abo-Elkhier M, Soliman MS. Superplastic characteristics of fine-grained 7475 aluminum alloy. *J Mater Eng Perform.* 2006;15:76–80.
- Guan Z, Ren M, Zhao P, et al. Constitutive equations with varying parameters for superplastic flow behavior of Al-Zn-Mg-Zr alloy. *Mater Des.* 2014;54:906–913.
- Wang XG, Li QS, Wu RR, et al. A review on superplastic formation behavior of Al alloys. *Adv Mater Sci Eng.*

2018. Article ID 7606140. <https://doi.org/10.1155/2018/7606140>
- [25] Pu H-P, Huang JC. Low temperature superplasticity in 8090 Al-Li alloys. *Scripta Metal Mater.* 1993;28:1125–1130.
- [26] Hsiao IC, Huang JC. Development of low temperature superplasticity in commercial 5083 Al-Mg alloys. *Scripta Mater.* 1999;40:697–703.
- [27] Park K-T, Hwang D-Y, Shin DH. Low-temperature superplastic behavior of a submicrometer-grained 5083 Al alloy fabricated by severe plastic deformation. *Metall Mater Trans A.* 2002;33:2859–2867.
- [28] Luo T, Ni DR, Xue P, et al. Low-temperature superplasticity of nugget zone of friction stir welded Al-Mg alloy joint. *Mater Sci Eng A.* 2018;727:177–183.
- [29] Ma ZY, Mishra RS. Development of ultrafine-grained microstructure and low temperature (0.48 Tm) superplasticity in friction stir processed Al-Mg-Zr. *Scripta Mater.* 2005;53:75–80.
- [30] Liu FC, Ma ZY, Chen LQ. Low-temperature superplasticity of Al-Mg-Sc alloy produced by friction stir processing. *Scripta Mater.* 2009;60:968–971.
- [31] Frost HJ, Ashby MF. *Deformation-mechanism maps: the plasticity and creep of metals and ceramics.* Oxford: Pergamon Press; 1982.
- [32] Kovács Z, Chinh NQ. Up-hill diffusion of solute atoms towards slipped grain boundaries: a possible reason of decomposition due to severe plastic deformation. *Scripta Mater.* 2020;188:285–289.
- [33] Chinh NQ, Szommer P, Horita Z, et al. Experimental evidence for grain boundary sliding in ultrafine-grained aluminum processed by severe plastic deformation. *Adv Mater.* 2006;18:34–39.
- [34] Valiev RZ, Murashkin MY, Kilmametov A, et al. Unusual super-ductility at room temperature in an ultrafine-grained aluminum alloy. *J Mater Sci.* 2010;45:4718–4724.
- [35] Chinh NQ, Valiev RZ, Sauvage X, et al. Grain boundary phenomena in an ultrafine-grained Al-Zn alloy with improved mechanical behavior for micro-devices. *Adv Eng Mater.* 2014;16:1000–1009.
- [36] Chinh NQ, Szommer P, Gubicza J, et al. Characterizing microstructural and mechanical properties of Al-Zn alloys processed by high-pressure torsion. *Adv Eng Mater.* 2020;22:1900672.
- [37] Straumal B, Valiev R, Kogtenkova O, et al. Thermal evolution and grain boundary phase transformations in severely deformed nanograined Al-Zn alloys. *Acta Mater.* 2008;56:6123–6131.
- [38] Edalati K, Horita Z, Valiev RZ. Transition from poor ductility to room-temperature superplasticity in a nanostructured aluminum alloy. *Sci Rep.* 2018;8:6740.
- [39] Gubicza J. *Defect structure and properties of nanomaterials.* Duxford: Woodhead Publishing; 2017.
- [40] Petrik MV, Kuznetsov AR, Enikeev NA, et al. Peculiarities of interactions of alloying elements with grain boundaries and the formation of segregations in Al-Mg and Al-Zn alloys. *Phys Met Metallogr.* 2018;119:607–612.
- [41] Koju RK, Mishin Y. Atomistic study of grain-boundary segregation and grain-boundary diffusion in Al-Mg alloys. *Acta Mater.* 2020;201:596–603.
- [42] Polmear IJ. *Light alloys: metallurgy of the light metals.* 3rd ed London: Arnold; 1995.
- [43] Azarniya A, Taheri AK, Taheri KK. Recent advances in ageing of 7xxx series aluminum alloys: a physical metallurgy perspective. *J Alloys Compd.* 2019;781:945–983.